Acta Pharmaceutica Sinica B 2022;12(4):1856–1870

Chinese Pharmaceutical Association
Institute of Materia Medica, Chinese Academy of Medical Sciences

Acta Pharmaceutica Sinica B

www.elsevier.com/locate/apsb
www.sciencedirect.com

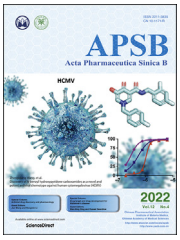

ORIGINAL ARTICLE

Blockade of deubiquitinase YOD1 degrades oncogenic PML/RARα and eradicates acute promyelocytic leukemia cells

Xuejing Shao[a,†], Yingqian Chen[a,†], Wei Wang[a], Wenxin Du[a], Xingya Zhang[a], Minyi Cai[a], Shaowei Bing[a], Ji Cao[a,c,d], Xiaojun Xu[b], Bo Yang[a,d], Qiaojun He[a,c,d], Meidan Ying[a,b,c,*]

[a]*Institute of Pharmacology and Toxicology, Zhejiang Province Key Laboratory of Anti-Cancer Drug Research, College of Pharmaceutical Sciences, Zhejiang University, Hangzhou 310058, China*
[b]*Children's Hospital, Zhejiang University School of Medicine, National Clinical Research Center for Child Health, Hangzhou 310052, China*
[c]*Cancer Center, Zhejiang University, Hangzhou 310058, China*
[d]*Innovation Institute for Artificial Intelligence in Medicine, Zhejiang University, Hangzhou 310058, China*

Received 20 July 2021; received in revised form 6 September 2021; accepted 28 September 2021

KEY WORDS

Acute promyelocytic leukemia;
PML/RARα;
Deubiquitinase;
YOD1;

Abstract In most acute promyelocytic leukemia (APL) cells, promyelocytic leukemia (PML) fuses to retinoic acid receptor α (RARα) due to chromosomal translocation, thus generating PML/RARα oncoprotein, which is a relatively stable oncoprotein for degradation in APL. Elucidating the mechanism regulating the stability of PML/RARα may help to degrade PML/RARα and eradicate APL cells. Here, we describe a deubiquitinase (DUB)-involved regulatory mechanism for the maintenance of PML/RARα stability and develop a novel pharmacological approach to degrading PML/RARα by inhibiting DUB. We utilized a DUB siRNA library to identify the ovarian tumor protease (OTU) family member

Abbreviations: APL, acute promyelocytic leukemia; ATO, arsenic trioxide; ATRA, all-*trans* retinoic acid; cAMP, cyclic adenosine monophosphate; EARD, endoplasmic reticulum-associated degradation; FLT3/ITD, internal tandem duplication within FLT3; G5, ubiquitin isopeptidase inhibitor I; *HOTAIRM1*, HOXA transcript antisense RNA myeloid-specific 1; JAMM, Jab1/Pab1/MPN domain-containing protease; LATS, large tumor suppressor kinase; MDM2, murine double minute 2; MINDY, motif-interacting with ubiquitin-containing novel DUB family; MJD, machado-Joseph domain-containing protease; OUT, ovarian tumor; PLZF, promyelocytic leukemia zinc finger; PML, promyelocytic leukemia; RARα, retinoic acid receptor α; RNF4, ring finger protein 4; S100A3, S100 calcium binding protein A3; TAZ, transcriptional co-activator with PDZ-binding motif; TGFβ, transforming growth factor β; TRIB3, tribbles pseudokinase 3; UCH, ubiquitin carboxyl terminal hydrolase; UCHL1, ubiquitin c-terminal hydrolase L1; USP, ubiquitin specific protease; YAP, yes-associated protein.

*Corresponding author. Tel./fax: +86 571 88208401.
E-mail address: mying@zju.edu.cn (Meidan Ying).
[†]These authors made equal contributions to this work.

Peer review under responsibility of Chinese Pharmaceutical Association and Institute of Materia Medica, Chinese Academy of Medical Sciences.

https://doi.org/10.1016/j.apsb.2021.10.020

Degradation;
Drug resistance;
Inhibitor;
Therapy

deubiquitinase YOD1 as a critical DUB of PML/RARα. Suppression of YOD1 promoted the degradation of PML/RARα, thus inhibiting APL cells and prolonging the survival time of APL cell-bearing mice. Subsequent phenotypic screening of small molecules allowed us to identify ubiquitin isopeptidase inhibitor I (G5) as the first YOD1 pharmacological inhibitor. As expected, G5 notably degraded PML/RARα protein and eradicated APL, particularly drug-resistant APL cells. Importantly, G5 also showed a strong killing effect on primary patient-derived APL blasts. Overall, our study not only reveals the DUB-involved regulatory mechanism on PML/RARα stability and validates YOD1 as a potential therapeutic target for APL, but also identifies G5 as a YOD1 inhibitor and a promising candidate for APL, particularly drug-resistant APL treatment.

1. Introduction

Acute promyelocytic leukemia (APL) is characterized by the t(15;17)(q24;q21) chromosomal translocation, which fuses promyelocytic leukemia (PML) to retinoic acid receptor α (RARα) and generates PML/RARα oncoprotein[1]. PML/RARα is a clinically acknowledged therapeutic target to cure APL. First, PML/RARα is considered to be critical for APL pathogenesis. The expression of PML/RARα is sufficient to initiate APL in mice[2,3], and the proliferation of APL-initiating cells depends on the expression of PML/RARα[4]. Second, PML/RARα is a useful diagnostic biomarker for APL, and its detection is performed because PML/RARα-driven APL tends to be sensitive to all-*trans* retinoic acid (ATRA) and arsenic trioxide (ATO), which are both targeted drugs to initiate PML/RARα proteolysis[1,5]. Thus, triggering the degradation of oncogenic PML/RARα has been considered as a successful strategy to treat APL.

After incorporation of ATRA and ATO into the APL management paradigms, the prognosis has dramatically improved for APL patients[6]. Nonetheless, significant challenges still remain. For instance, serious adverse events such as hepatotoxicity, gastrointestinal symptoms, water-sodium retention, and nervous system damage frequently occur in the clinical setting[6–8]. Furthermore, some patients develop resistance during therapy, and relapse and refractory responses are still observed in patients under treatment[9,10]. Studies incorporating genome sequencing analyses have demonstrated that genetic mutations in the PML moiety (*e.g.*, L218P and A216V) or RARα moiety (*e.g.*, ΔF286 and R276Q) of PML/RARα disrupt its binding to ATRA or ATO, thus hindering the subsequent degradation process, which ultimately leads to resistance to ATRA and ATO treatment[9–11]. Therefore, novel strategies to trigger PML/RARα degradation would be valuable for treating APL, particularly drug-resistant APL patients.

PML/RARα is a relatively stable oncoprotein with a 24-h half-life for degradation in APL cells[12]. The mechanisms currently recognized for regulating the stability of PML/RARα were discovered through treatment with ATRA and ATO. Specifically, ATO destabilizes PML/RARα through the ubiquitination proteasome pathway, by conjugating SUMO to the PML portion and recruiting the ubiquitin ligase ring finger protein 4 (RNF4)[13,14]. ATRA binds to the RARα portion and triggers the ligand-dependent degradation of PML/RARα[15,16]. Autophagic degradation of PML/RARα is also activated upon exposure to ATRA and ATO[17]. Cyclic adenosine monophosphate (cAMP)[4,18], S100 calcium binding protein A3 (S100A3)[19] and lncRNA HOXA transcript antisense RNA myeloid-specific 1 (*HOTAIRM1*)[20] also affect the ATRA- and ATO-induced degradation of PML/RARα. However, the regulatory mechanisms contributing to the stability of PML/RARα under pathological conditions remain largely unknown. Although additional studies have clarified roles of some signaling factors [*e.g.*, tribbles pseudokinase 3 (TRIB3) and microRNA 125b-1] in regulating the stability of PML/RARα under pathological conditions, these factors are relatively difficult to target with inhibitors[12,21]. Thus, novel druggable targets that can destroy PML/RARα stability remain to be explored.

Deubiquitinases (DUBs) specifically deconjugate the ubiquitin chain from substrates, thus realizing the purpose of maintaining protein stability[22,23]. Accumulating evidence implicates DUBs as remarkable drug targets for cancers[24]. First, DUB deregulation has been reported to contribute to the accumulation of key oncoproteins, such as ubiquitin specific protease 7 (USP7) deubiquitinates and stabilizes N-Myc in neuroblastoma[25], and USP28 is required for MYC stability[26]. And some DUBs have also been described to manifest oncogenic activities, such as ubiquitin c-terminal hydrolase L1 (UCHL1) is identified as a candidate oncoprotein that promotes transforming growth factor β (TGFβ)-induced breast cancer metastasis[27]. Second, DUBs possess well-defined catalytic clefts with known enzymatic functions, which enables the identification of small-molecule inhibitors for DUBs. Third, DUBs often show specificity for targeted substrates[24]. Thus, we suggest that the high stability of PML/RARα may result from the dysregulation of its specific DUB, and targeting this DUB promises to provide an effective approach for inducing PML/RARα degradation to achieve ideal therapeutic effects in APL patients.

In the present study, we validate the deubiquitinase of the ovarian tumor protease (OTU) family YOD1 (also known as OTUD2 or OTU1) as a specific DUB that upregulates the protein stability of PML/RARα. And we identify ubiquitin isopeptidase inhibitor I (G5) as the first YOD1 inhibitor to be a promising candidate for APL, particularly drug-resistant APL treatment.

2. Materials and methods

2.1. Cells and culture

Human embryonic kidney HEK-293T and 293FT cell lines were supplied by Invitrogen (Grand Island, NY, USA). Monkey kidney COS-7, human H1299 and the human myeloid leukemia (non-APL) U937 and HL60 cell lines were purchased from the Shanghai Institute of Biochemistry and Cell Biology (Shanghai, China). The NB4 human myeloid leukemia cell line was kindly gifted from Dr. Lingtao Wu (University of Southern California,

CA, USA), the NB4R1 cell line was a kind gift from Dr. He Huang (Zhejiang University, Hangzhou, China) and the NB4R2 cell line was kindly provided by Dr. Jian Zhang (Shanghai Jiao Tong University, Shanghai, China). Primary APL blasts (Leu-1−12) extracted from the bone marrow of patients (Children's Hospital of Zhejiang University and First Affiliated Hospital of Zhejiang University, Hangzhou, China) were isolated using Ficoll-Paque PREMIUM (Cytiva). Written informed consents from patients and approval from the Institutional Research Ethics Committee of the hospital were obtained before the use of these clinical materials for research purposes.

Primary patient blasts (Leu-1−12) and normal human HSCs were cultured in IMDM medium supplemented with recombinant human SCF (50 ng/mL; R&D Systems), recombinant human IL-3 (10 ng/mL; R&D Systems), recombinant human IL-6 (5 ng/mL; R&D Systems), hydrocortisone (10 μmol/L; Sigma−Aldrich, St. Louis, MO, USA), L-glutamine (2 mmol/L), 20% fetal bovine serum (Gibco BRL) and 1% penicillin/streptomycin. Human myeloid leukemia (NB4, NB4R1, NB4R2 and U937 cells) and H1299 cell lines were cultured in RPMI 1640 medium, HL60 cell line was cultured in IMDM medium, and HEK-293T, 293FT and COS-7 cells were cultured in Dulbecco's modified Eagle's medium (DMEM). All of the media were supplemented with 10% fetal bovine serum (Gibco BRL) and 1% penicillin/streptomycin. All cell lines were maintained at 37 °C in a humidified atmosphere containing 5% CO_2 and passaged for a maximum of 2 months. All cell lines were routinely tested for mycoplasma using a Mycoplasma Detection Kit (Bimake) and authenticated utilizing short tandem repeat (STR) profiling every 6 months. Primary APL blasts (Leu-1−12) were cultured in IMDM supplemented with human SCF (50 ng/mL; PeproTech), IL-3 (10 ng/mL; PeproTech), IL-6 (5 ng/mL; PeproTech), hydrocortisone (1 μmol/L; Sigma−Aldrich), β-mercaptoethanol (100 μmol/L; Sigma−Aldrich), L-glutamine (2 mmol/L), 20% fetal bovine serum (Gibco BRL) and 1% penicillin/streptomycin.

2.2. Plasmids, reagents and antibodies

The full-length coding sequences for PML/RARα [long form (L) and short form (S)] were synthesized and subcloned into the pCDNA3.0 and pCDH plasmids. The firefly sequence was amplified from the pGL4 plasmid and subsequently subcloned into the pCDNA3.0-PML/RARα plasmid. Human YOD1 was amplified from the HEK-293T cDNA library and subcloned into a pCDNA3.0 plasmid. Drug-resistant PML/RARα mutants (ΔF286, R276Q, A216V and L218P) and a YOD1 mutant (C160S) were produced by site-directed mutagenesis. The packaging plasmid pRΔ8.9 and envelope plasmid pMD.G were kindly provided by Dr. D.B. Kohn (University of Southern California). The shRNA oligonucleotides targeting *YOD1*, *USP28* and *USP37* (Supporting Information Table S1) were annealed and cloned into pLKO.1 vector with AgeI/EcoRI sites.

ATRA and ATO was purchased from Sigma−Aldrich. Proteasome inhibitor MG132 was purchased from Selleck Chemicals. Ubiquitin isopeptidase inhibitor I, also known as G5, and EOAI3402143 were supplied by MedChemExpress (USA). Spautin-1 was purchased from TargetMol (Shanghai, China). ATRA was dissolved in ethanol. ATO was dissolved in distilled water. MG132, G5, EOAI3402143 and spautin-1 were dissolved in DMSO. In all experiments, the final solvent concentration was ≤0.1% (*v*/*v*).

Antibodies against YOD1 (25370-1-AP) were purchased from Proteintech. Antibodies against PML (db9346), HA (db2603), β-actin (db10001) and GAPDH (db106) were purchased from Diagbio. The anti-Flag antibody (HOA012FL01) was purchased from HuiOu Biotechnology. The anti-His antibody (R130420) was purchased from HuaBio.

2.3. DUBs siRNA library screening

HEK-293T cells were cotransfected with PML/RARα-*Firefly*, *Renilla* and DUB siRNAs (Dharmacon) per well in the presence of jetPrime (Polyplus). After 36 h, the cell lysate was analyzed with a Dual Luciferase Reporter Assay System (Promega). Relative firefly expression was determined as the ratio of *Firefly*-to-*Renilla* luciferase activity. The fold change of the relative firefly expression was normalized to that of the scramble control.

2.4. Lentivirus production and transduction

Virus production, titration and transduction were performed as described previously[28].

2.5. Real-time PCR

Real-time PCR was used to detect the mRNA levels of *PML/RARA* and *YOD1*. *GAPDH* was used as an internal standard. The primers used are shown in Supporting Information Table S2.

2.6. Immunoprecipitation

When detecting the interaction between PML/RARα and YOD1, cells were lysed in RIPA lysis buffer (50 mmol/L Tris-base, 150 mmol/L NaCl, 1% Triton X-100, 0.1% SDS, and 0.5% sodium deoxycholate, pH = 7.4), containing leupeptin, PMSF, and Na_3VO_4 for 30 min on ice, then centrifuged at 16,363×*g* for 30 min at 4 °C. To observe the polyubiquitination of PML/RARα, cells were lysed in 4% SDS buffer (4% SDS, 150 mmol/L NaCl and 50 mmol/L triethylamine, pH = 8.0). Then, the cell lysate was incubated with a 30 μL suspension of beads at 4 °C overnight. Finally, the beads were washed five times with wash buffer (50 mmol/L Tris-HCl, 150 mmol/L NaCl, and 1% NP40, pH = 8.0) before boiling. The boiled samples were then separated by SDS-PAGE and subjected to immunoblotting analysis with the indicated antibodies.

2.7. In vitro ubiquitination assay

COS7 cells were cotransfected with pCDNA3.0-PML/RARα-HA (L, S or mutant) and PRK5-His-Ub plasmid. After 36 h, cells were treated with MG132 (10 μmol/L) for 8 h before harvest, followed by cell lysis in 4% SDS buffer (4% SDS, 150 mmol/L NaCl, and 50 mmol/L triethylamine, pH = 8.0). Then, ubiquitinated PML/RARα-HA (L, S or mutant) was pulled down by immunoprecipitation with HA beads and subsequently incubated with recombinant wild-type GST-YOD1 or mutant GST-YOD1(C160S) at 37 °C for 6 h. When detecting the effect of DUB inhibitors, recombinant wild-type GST-YOD1 or mutant GST-YOD1 (C160S) was preincubated with different DUB inhibitors separately at 37 °C for 1 h. The ubiquitination of PML/RARα was detected by Western blotting with a His antibody.

2.8. Cellular proliferation analysis

The cell count and viability were determined with manual counting by the trypan blue (Sigma) exclusion method in Burker chambers. Nonviable and dead cells were identified as those that had taken up trypan blue dye.

2.9. Soft agar formation assay

The wells of a 6-well plate were coated with 2 mL of 0.5% soft agar (Sigma), and the agar mixture was allowed to solidify at room temperature. Then, the cells were mixed in 0.3% soft agar to plate the upper layer. After the agar solidified, the cultures were placed into a humidified cell culture incubator set to 37 °C. The cells were incubated several days until colonies formed. Then, nitrotetrazolium blue chloride was added to each well to stain the cells. The cell number used for colony formation assay is 1000 (NB4 cells) or 2000 (NB4R1 and NB4R2 cells) cells per well. The stained clones were photographed using a camera, and were automatically counted using ImageJ.

Relative clonal formation rate (%) = (The number of clones in shYOD1 group/The number of clones in the shCtrl group) × 100. (1)

2.10. Cell apoptosis analysis

The apoptosis quantification was detected by PI/Annexin V-staining, and Annexin V-stained (PI^-/Annexin V^+ and PI^+/Annexin V^+) cells were analyzed to measure the cell apoptosis rate.

2.11. Cell differentiation analysis

To assess CD11b expression, a fluorochrome conjugate of monoclonal antibody was used to detect CD11b expression following the protocol from the manufacturer (BD Biosciences).

2.12. A cell-based YOD1 inhibitor screening assay

H1299 cells stably expressing PML/RARα were seeded into 24-well plates, and the next day, the cells were exposed to the library of 31 reported DUB inhibitors at a concentration of 5 μmol/L for 12 h. Then, the protein levels of PML/RARα were assessed by Western blotting. The relative protein levels of PML/RARα were determined as the ratio of PML/RARα to GAPDH, and the ratio of PML/RARα/GAPDH was normalized to level of the solvent control.

2.13. Recombinant YOD1 purification

Plasmids containing GST-YOD1 or GST-YOD1 (C160S) were transformed into *Escherichia coli* BL21 (DE3) cells. After induction with isopropyl β-D-thiogalactoside (IPTG), the bacteria in buffer (137 mmol/L NaCl, 2.7 mmol/L KCl, 1.76 mmol/L KH_2PO_4 and 10 mmol/L $Na_2HPO_4 \cdot 12H_2O$, pH = 7.4) were lysed by a High-pressure Bacteria Breaker (Union Biotech). The GST-fusion protein was purified using a GST affinity column (GE healthcare). The eluted protein was dialyzed overnight in 3 L of dialysis buffer (50 mmol/L Tris-HCl, 150 mmol/L NaCl, 0.5 mmol/L EDTA and 10% glycerol, pH = 8.0) at 4 °C.

2.14. Animal studies

To generate an orthotopic xenograft model, NB4 or NB4R1 cells were transduced with shCtrl or shYOD1 (#1 and #2) lentivirus. The mice were sublethally pretreated with cyclophosphamide. Then, NB4 cells (1×10^7 cells) or NB4R1 cells (2×10^7 cells) were injected into 6- to 7-week-old NOD/SCID mice (SLRC Laboratory Animal Inc.) *via* the tail vein. Some mice were killed on the indicated days (30 days for those implanted with NB4 cells) after transplantation. First, the bone marrow cells were stained by Wright−Giemsa to determine the tumor burden in the mice. Next, the leukemic cells were confirmed by analyzing the proportion of human CD45-positive and mouse CD45-negative ($hCD45^+mCD45^-$) cells in the bone marrow as described previously[28]. It is reported that successful leukemia engraftment was defined by the presence of > 1% human $CD45^+$ murine $CD45^-$ cells in the recipient BM or PB[29−31]. For other mice, the survival times were recorded.

To perform the xenograft experiment, 2×10^7 NB4R2 cells were injected subcutaneously into 4- to 5-week-old female nude mice (SLRC Laboratory Animal Inc.). When the tumors reached a volume from 200 to 400 mm^3, the mice were allocated by tumor volume into four groups. The mice were treated with G5 (20 or 40 mg/kg; i.v.) every other day or with ATRA (20 mg/kg; i.g.) every other day for 13 days. The tumor volume was recorded until the animals were sacrificed.

The Animal Research Committee at Zhejiang University approved all animal studies and animal care was provided in accordance with the institutional guidelines.

2.15. Statistical analysis

For all parameters measured, the values for all samples under different experimental conditions were averaged, and the standard deviation (SD) or Standard error (SE) was calculated. The statistical significance of differences between groups was determined by unpaired two-tailed Student's *t*-test analysis, one-way analysis of variance (ANOVA) with Tukey's tests or Log-rank test. The results are considered significant when $P < 0.05$ (n.s., $P > 0.05$; $^*P < 0.05$; $^{**}P < 0.01$; and $^{***}P < 0.001$).

3. Results

3.1. YOD1 is identified as a key DUB to modulate the stability of the PML/RARα protein

To identify the potential DUBs modulating the stability of PML/RARα, we utilized a cell-based dual-luciferase reporter screening assay combined with a siRNA library which targeted 98 recognized human DUBs. As shown in Fig. 1A, PML/RARα-*Firefly* was used to evaluate the PML/RARα protein levels, and *Renilla* served as the internal control. After cells were transfected with the DUB siRNA library for 36 h, the firefly and *Renilla* luciferase activity levels were measured and used to calculate the relative *Firefly* activity. The results show that the siRNAs targeting three DUBs (*USP28*, *USP37* and *YOD1*) significantly attenuated the protein level of PML/RARα, by approximately 50% (Fig. 1B). To further validate the regulatory effect of these three DUB candidates on the protein abundance of PML/RARα, we constructed two independent shRNAs targeting each DUB. The results demonstrate that the protein level of PML/RARα was obviously

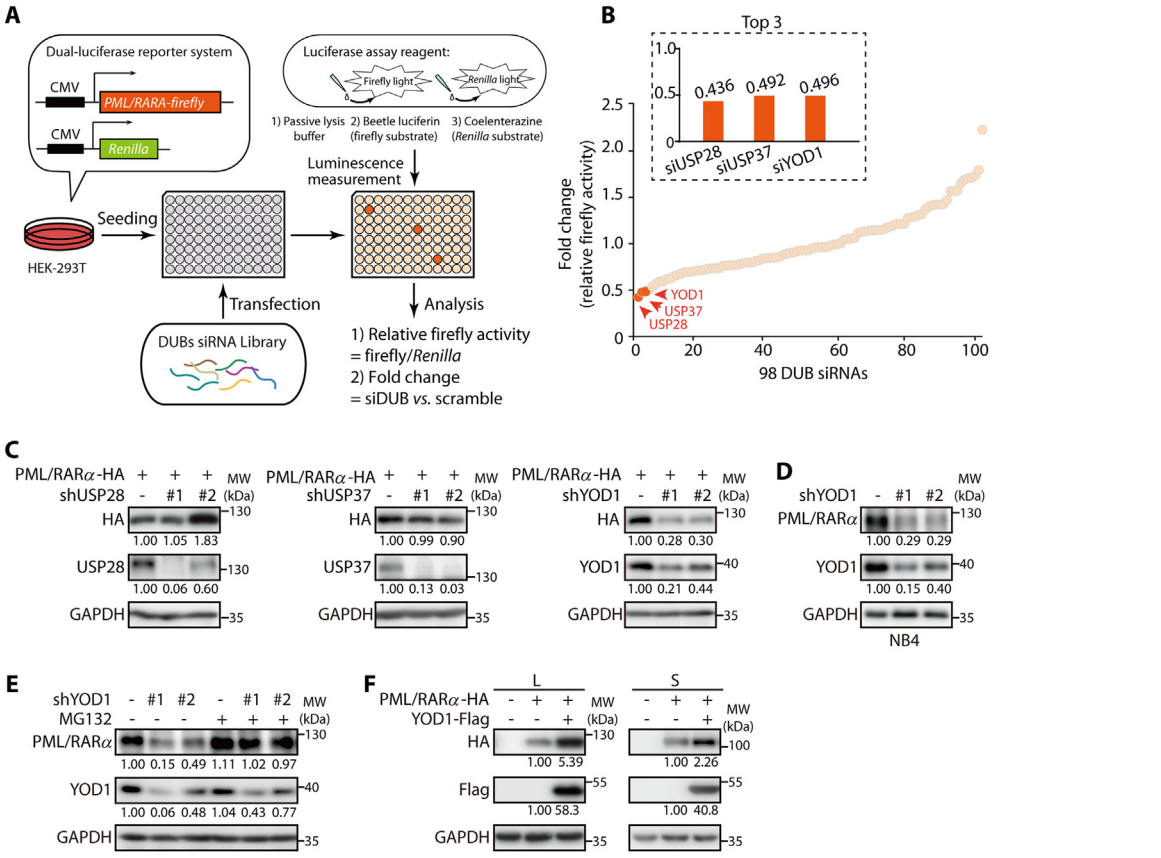

Figure 1 YOD1 is identified as a key deubiquitinase to modulate the stability of the PML/RARα protein. (A) Schematic diagram of the dual-luciferase reporter system utilized to screen deubiquitinases (DUBs) modulating the stability of PML/RARα. (B) Relative firefly activity of PML/RARα. pCDNA3.0-PML/RARα-firefly-overexpresssing HEK-293T cells were transfected with siRNAs targeting 98 DUBs. The inhibition ratios of the top 3 most effective DUB siRNAs that significantly reduced the relative *Firefly* were indicated. (C) Effect of USP28, USP37 and YOD1 knockdown on the protein level of PML/RARα. PML/RARα-overexpressing HEK-293T cells were infected with shUSP28, shUSP37 or shYOD1 lentivirus, and the protein levels of PML/RARα were evaluated by Western blotting. (D) Effect of shYOD1 on the protein level of endogenous PML/RARα. NB4 cells were infected with lentivirus-shYOD1 (#1 and #2) for 72 h, and then, the protein expression levels of PML/RARα and YOD1 were measured by Western blotting. (E) Effect of MG132 on the shYOD1-induced PML/RARα decline. NB4 cells infected with shYOD1 (#1 and #2) were treated with or without MG132 (40 nmol/L) for 72 h, and then subjected to Western blotting. (F) Effect of YOD1 on the protein levels of exogenous long form (L) and shot form (S) of PML/RARα as determined by Western blotting. HEK-293T cells were cotransfected with PML/RARα-HA (L or S) and YOD1-Flag plasmids. (C)−(F) Data are performed at least three individual experiments and one representative image is shown.

reduced by shYOD1, while it was not reduced by shUSP28 and moderately decreased by shUSP37 (Fig. 1C). Meanwhile, YOD1 suppression also decreased the level of the short isoform of PML/RARα [PML/RARα (S)], which is another major isoform of PML/RARα, differing from PML/RARα (L) that mainly used in this article (Supporting Information Fig. S1A). These results collectively indicate that *YOD1* silencing can downregulate the protein level of PML/RARα, inspiring us to further study the role of YOD1 in regulating the stability of PML/RARα.

Next, we evaluated the regulatory effect of YOD1 in the cellular context of APL. As expected, YOD1 knockdown significantly decreased the level of endogenous PML/RARα in the NB4 cells (Fig. 1D). More importantly, the shYOD1-induced decline in PML/RARα protein level was completely abolished by the proteasome inhibitor MG132 (Fig. 1E), whereas *PML/RARA* mRNA level was not affected by shYOD1 (Fig. S1B), indicating that YOD1 regulates the protein level of PML/RARα in a proteasome-dependent manner. Consistent with this finding, overexpression of YOD1 obviously increased the protein levels of both PML/RARα (L) and PML/RARα (S) (Fig. 1F). These results strongly indicate that YOD1 functions as a critical regulator for the ubiquitination proteasome pathway-dependent degradation of PML/RARα.

3.2. YOD1 silencing decreases the protein levels of drug-resistant PML/RARα mutants

Since the regulatory effect of YOD1 on the protein stability of PML/RARα has been validated, we wonder whether YOD1 can also manipulate the stability of drug-resistant PML/RARα mutants. First, two ATRA-resistant APL cell strains (NB4R1 and NB4R2 cells) harboring mutated PML/RARα were obtained[32]. Western blot analysis confirmed that ATRA significantly degraded wild-type PML/RARα in NB4 cells, whereas the protein levels of mutated PML/RARα (ΔF286) in NB4R1 cells were partially decreased and those of mutated PML/RARα (Q411X) in NB4R2 cells were negligibly affected by

ATRA (Fig. 2A, Left). In contrast to the effect of ATRA, shYOD1 not only caused a notable reduction in the wild-type PML/RARα level in NB4 cells but also almost completely eliminated drug-resistant PML/RARα mutants in NB4R1 and NB4R2 cells (Fig. 2A, Right). These results provide the possibility that silencing YOD1 can degrade drug-resistant PML/RARα mutants to overcome ATRA resistance.

To further evaluate the modulatory effect of shYOD1 on various drug-resistant PML/RARα mutants, we introduced more ATRA- and ATO-resistant forms of PML/RARα with distinct clinical missense mutations detected in APL patients. As shown in Fig. 2B, in contrast to wild-type PML/RARα, the two ATRA-resistant PML/RARα mutants (ΔF286 and R276Q) showed little responsiveness to ATRA-induced degradation. By contrast, when exposed to shYOD1, both wild-type PML/RARα and ATRA-resistant PML/RARα mutants (ΔF286 and R276Q) were significantly decreased. Meanwhile, although ATO-resistant forms of PML/RARα (A216V and L218P) failed to degrade upon ATO treatment, their protein abundance were also effectively diminished by shYOD1 (Fig. 2C). These results further confirm the

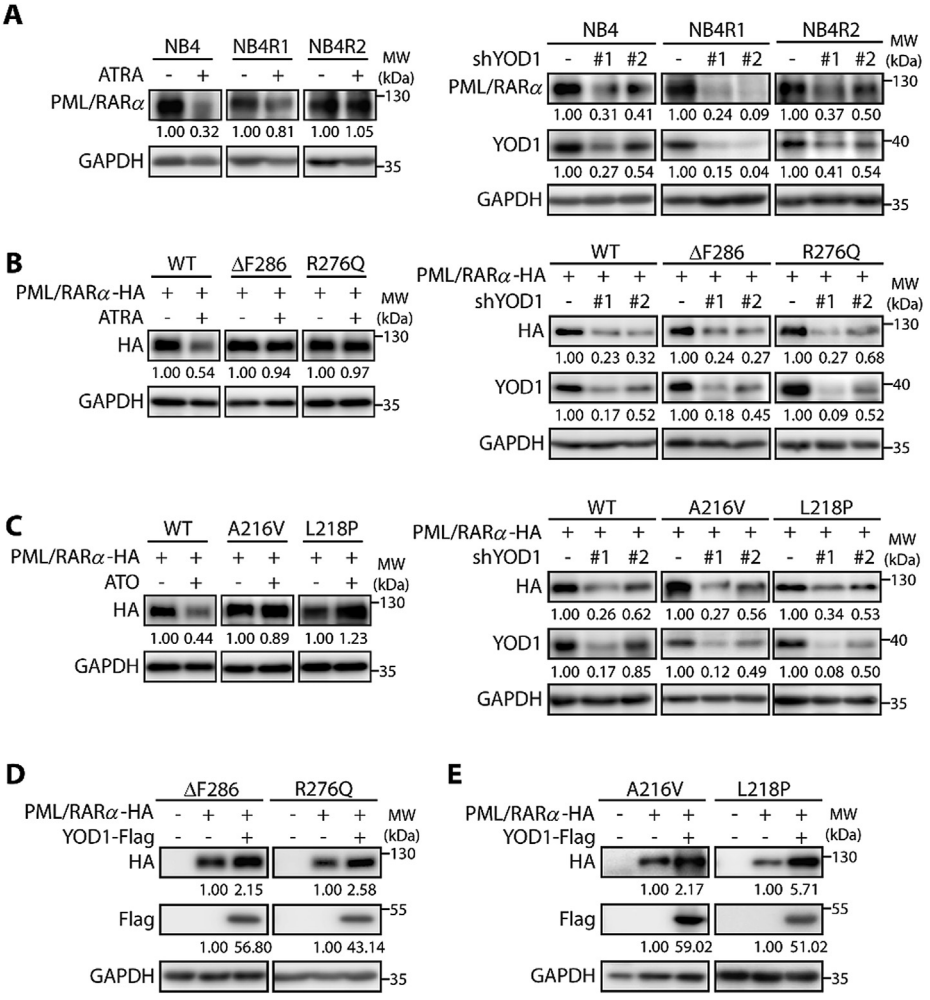

Figure 2 YOD1 silencing decreases the protein levels of drug-resistant PML/RARα mutants. (A) The effect of shYOD1 on endogenous PML/RARα in drug-resistant APL cells. Protein expression level of PML/RARα in NB4, NB4R1, and NB4R2 cells after treatment with 0.1 μmol/L ATRA for 72 h, as evaluated by Western blotting (Left). Western blotting of PML/RARα and YOD1 in NB4, NB4R1, and NB4R2 cells infected with lentivirus-shYOD1s for 72 h (Right). (B) The effect of shYOD1 on exogenous ATRA-resistant PML/RARα mutants. HEK-293T cells stably overexpressed PML/RARα (WT)-HA, PML/RARα (ΔF286)-HA or PML/RARα (R276Q)-HA. The cells were treated with 5 μmol/L ATRA for 12 h (Left). Cells were infected with shYOD1 (#1 and #2) for 72 h (Right). (C) The effect of shYOD1 on exogenous ATO-resistant PML/RARα mutants. HEK-293T cells stably overexpressed PML/RARα (WT)-HA, PML/RARα (A216V)-HA or PML/RARα (L218P)-HA. The cells were treated with 5 μmol/L ATO for 12 h (Left). Cells were infected with shYOD1 (#1 and #2) for 72 h (Right). (D) Effect of YOD1 overexpression on the protein levels of exogenous PML/RARα mutants (ΔF286 and R276Q). HEK-293T cells were cotransfected with YOD1-Flag and PML/RARα (ΔF286)-HA or PML/RARα (R276Q)-HA plasmids, and the levels of exogenous PML/RARα mutants were determined by Western blotting. (E) Effect of YOD1 overexpression on the protein levels of exogenous PML/RARα mutants (A216V and L218P). HEK-293T cells were cotransfected with YOD1-Flag and PML/RARα (A216V)-HA or PML/RARα (L218P)-HA plasmids, and the levels of exogenous PML/RARα mutants were determined by Western blotting. (A)−(E) Data are performed at least three individual experiments and one representative image is shown.

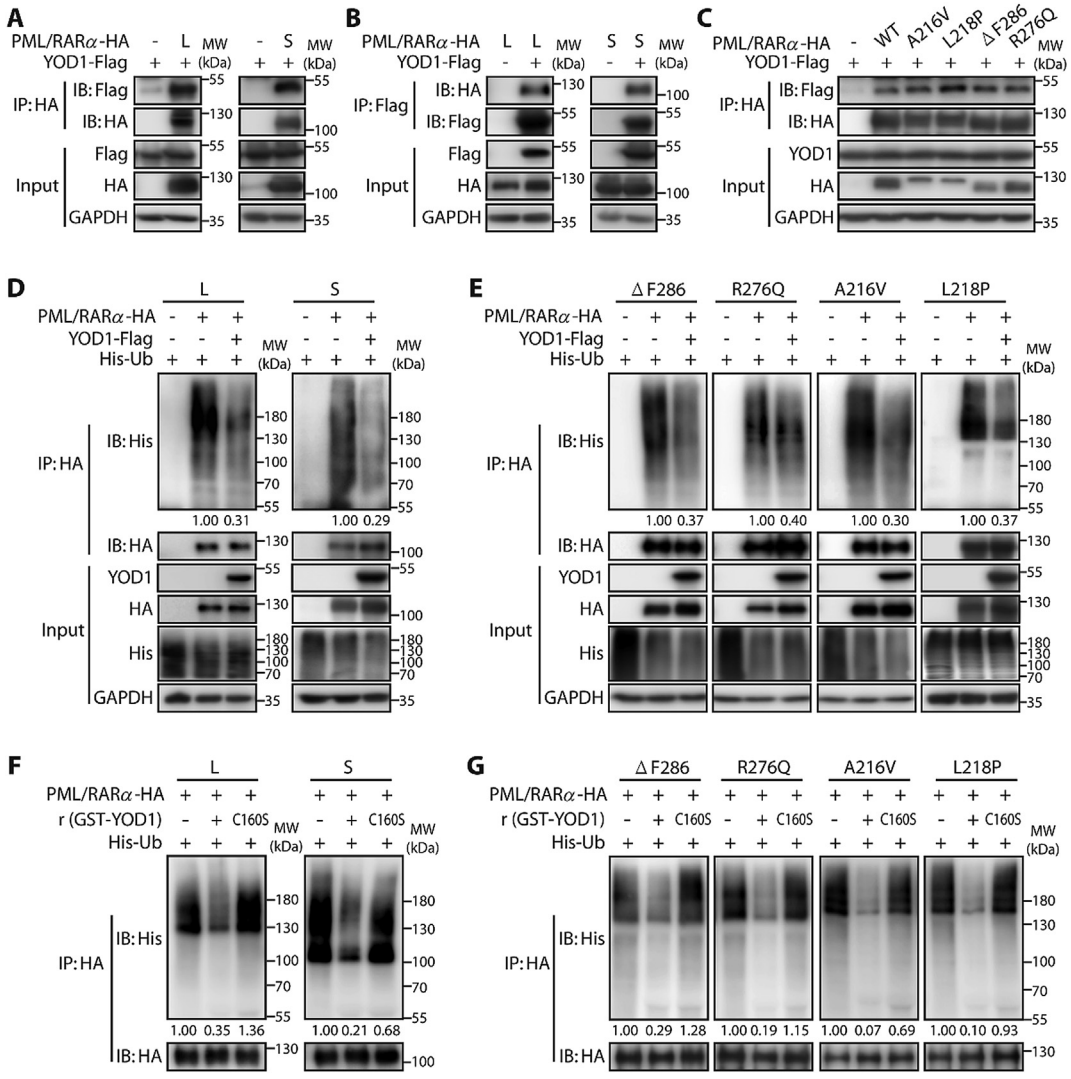

Figure 3 YOD1 deubiquitinates wild-type PML/RARα and its drug-resistant mutants. (A) and (B) The physical interactions between PML/RARα and YOD1 detected by immunoprecipitation. HEK-293T cells were cotransfected with PML/RARα-HA (L or S) and YOD1-Flag as indicated. Cell extracts were immunoprecipitated with HA beads, and anti-Flag antibody was used for detection. (A). Cell extracts were immunoprecipitated with Flag beads followed by examination with anti-HA antibody (B). (C) The interactions between PML/RARα drug-resistant mutants (ΔF286, R276Q, L218P and A216V) and YOD1 were detected by immunoprecipitation. HEK-293T cells overexpressed mutant PML/RARα-HA and YOD1-Flag, extracts from these cells were subjected to immunoprecipitation with anti-HA antibody, and the interacting proteins were determined by Western blotting with anti-Flag antibody. (D) The deubiquitinating effect of YOD1 on PML/RARα in cells. COS-7 cells were cotransfected with PML/RARα-HA (L or S), YOD1-Flag and His-Ub as indicated and then treated with MG132 (10 μmol/L) for 8 h. Cell extracts were immunoprecipitated with anti-HA beads, and the ubiquitination of PML/RARα was detected by Western blotting with anti-His antibody. (E) The deubiquitinating effect of YOD1 on PML/RARα drug-resistant mutants (ΔF286, R276Q, L218P and A216V) in cells. COS-7 cells were cotransfected with mutant PML/RARα-HA, YOD1-Flag and His-Ub as indicated and then treated with MG132 (10 μmol/L) for 8 h. After immunoprecipitation with anti-HA beads, the ubiquitination of PML/RARα drug-resistant mutants were examined by Western blotting with anti-His antibody. (F) The effect of YOD1 on the ubiquitination of PML/RARα *in vitro*. (G) The effect of YOD1 on the ubiquitination of PML/RARα drug-resistant mutants (ΔF286, R276Q, L218P and A216V) *in vitro*. (F) and (G) COS-7 cells were cotransfected with PML/RARα-HA and His-Ub, and were treated with MG132 (10 μmol/L) for 8 h. Then, ubiquitinated PML/RARα was enriched with anti-HA beads and subsequently incubated with recombinant wild-type GST-YOD1 or the catalytically inactive mutant GST-YOD1 (C160S). The ubiquitination of PML/RARα was detected by Western blotting with anti-His antibody. (A)−(G) Data are performed at least three individual experiments and one representative image is shown.

modulatory effect of shYOD1 on various drug-resistant PML/RARα mutants.

Furthermore, experiments were performed to determine the effect of YOD1 overexpression on drug-resistant PML/RARα mutants. Similar accumulation of PML/RARα protein levels induced by YOD1 overexpression was also observed on all four drug-resistant PML/RARα mutants, including the ATRA-resistant mutants (ΔF286 and R276Q) and the ATO-resistant mutants

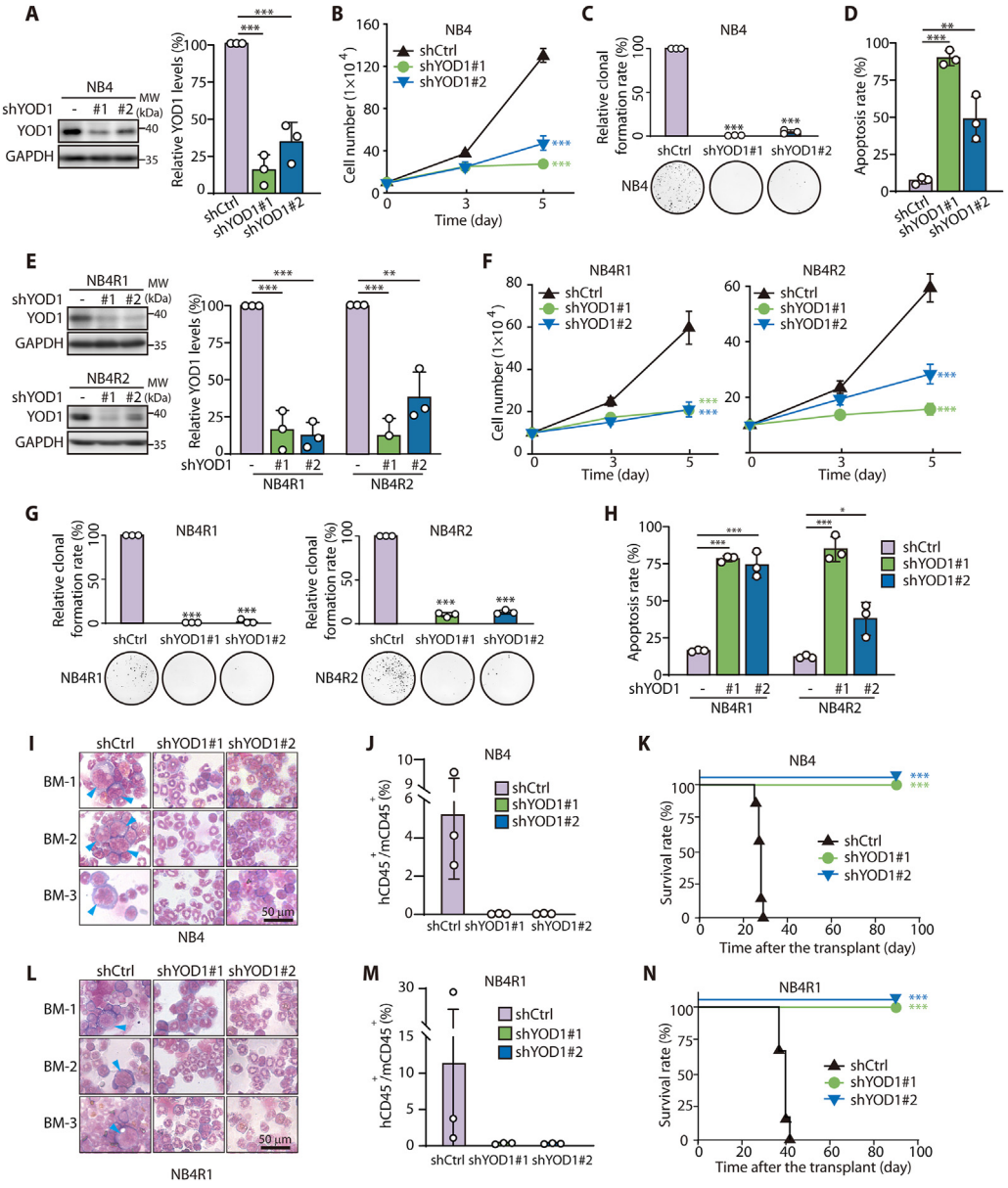

Figure 4 Depletion of YOD1 leads to effective APL eradication *in vitro* and *in vivo*. (A) The silencing efficiency of different shRNAs (#1 and #2) against YOD1 in NB4 cells. The protein levels of YOD1 were measured by Western blotting. (B) Proliferation of NB4 cells infected with lentivirus-shYOD1 (#1 and #2), as determined by trypan blue exclusion test for the indicated times. (C) Colony formation assay of NB4 cells transduced with lentivirus-shYOD1 (#1 and #2). 1000 cells were seeded per well and the colony numbers were counted after several days. Relative clonal formation rate is the ratio of the number of clones in each group to the number of clones in the shCtrl group. (D) Fluorescence-activated cell sorting (FACS) quantification of apoptosis with $PI^-/Annexin\ V^+$ or $PI^+/Annexin\ V^+$ NB4 cells. NB4 cells were infected with shYOD1 for 5 days. (E) The silencing efficiency of different shRNAs (#1 and #2) against YOD1 in NB4R1 and NB4R2 cells. (F) Cell proliferation of NB4R1 and NB4R2 cells infected with lentivirus-shYOD1s, as determined by trypan blue exclusion test for the indicated times. (G) Colony formation assay of NB4R1 and NB4R2 cells transduced with lentivirus-shYOD1s. 2000 cells were seeded per well and the colony numbers were counted after several days. Relative clonal formation rate is calculated as 4C. (H) FACS quantification of apoptosis with $PI^-/Annexin\ V^+$ or $PI^+/Annexin\ V^+$ NB4R1 and NB4R2 cells. Cells were infected with shYOD1s for 5 days. (A)−(H) Data are presented as mean ± SD ($n = 3$); $^*P < 0.05$, $^{**}P < 0.01$, and $^{***}P < 0.001$ *vs.* shCtrl or indicated. The significance analysis was conducted by one-way ANOVA analysis. (I)−(K) The effect of YOD1 on the NB4 tumor burden of NOD/SCID mice. NOD/SCID mice were transplanted with NB4-shCtrl or NB4-shYOD1 (#1 and #2) cells. (I) and (J) The mice were sacrificed 30 days after cell transplantation to detect the APL burden in bone marrow. Cell morphological analysis of bone marrow cells obtained and subjected to Wright−Giemsa staining (I). Blue arrow: APL blasts. Scale bar: 50 μm. The population of human CD45-positive and mouse CD45-negative ($hCD45^+mCD45^-$) leukemia cells in the bone marrow of NOD/SCID mice were determined (J). Data are presented as mean ± SD ($n = 3$); $^{***}P < 0.001$ *vs.* shCtrl. The significance analysis was conducted by one-way ANOVA analysis. (K) The survival times of the NOD/SCID mice were recorded ($n = 7$); $^{***}P < 0.001$ *vs.* indicated. The significance analysis was conducted by Log-rank test. (L)−(N) The effect of YOD1 on the NB4R1 tumor burden of NOD/SCID mice. NOD/SCID mice were transplanted with NB4R1-shCtrl or NB4R1-shYOD1 (#1 and #2) cells. (L) Cell morphological analysis of bone marrow cells. (M) The population of $hCD45^+mCD45^-$ leukemia cells in the bone marrow. Data are presented as mean ± SD ($n = 3$). (N) The survival times of the NOD/SCID mice were recorded ($n = 6$); $^{***}P < 0.001$ *vs.* indicated. The significance analysis was conducted by Log-rank test.

(L218P and A216V) (Fig. 2D and E). Taken together, these results strongly indicate that YOD1 regulates the stability of both the wild-type and mutant forms of PML/RARα.

3.3. *YOD1 deubiquitinates wild-type PML/RARα and its drug-resistant mutants*

Given that YOD1 serves as a critical regulator of the stability of wild-type PML/RARα and its drug-resistant mutants, we next determined the mechanisms underlying this modulatory effect. First, we performed a co-immunoprecipitation assay to examine the physical interaction between YOD1 and PML/RARα. Results reveal that exogenously expressed YOD1-Flag and PML/RARα-HA (both the L and S isoforms) were robustly coprecipitated (Fig. 3A). In a reciprocal immunoprecipitation experiment, overexpressed HA-tagged PML/RARα could also be detected in the immunocomplex of YOD1-Flag (Fig. 3B). Similarly, different drug-resistant PML/RARα mutants were also in contact within YOD1, as confirmed by immunoprecipitation (Fig. 3C). Thus, these results indicate that YOD1 physically interacts with both the wild-type and mutant forms of PML/RARα.

DUBs enhance the stability of proteins by directly deconjugating the ubiquitin chain from substrates to enable their escape from proteasomal degradation. Thus, we first performed a deubiquitination assay in cells, and the results show that overexpression of YOD1 significantly reduced the ubiquitination level of wild-type PML/RARα, including both L and S isoforms (Fig. 3D). In line with these results, YOD1 also notably downregulated the ubiquitination levels of drug-resistant PML/RARα mutants (ΔF286, R276Q, L218P and A216V) (Fig. 3E), strongly supporting that YOD1 may deubiquitination of PML/RARα. Therefore, an *in vitro* deubiquitination assay was utilized to validate the deubiquitinating effect of YOD1 on PML/RARα. We pulled down ubiquitinated PML/RARα proteins from cells and incubated them with recombinant wild-type YOD1 or its catalytically inactive mutant YOD1 (C160S) in a cell-free system. Results reveal that purified YOD1 effectively deubiquitinated PML/RARα *in vitro*, while YOD1(C160S) failed to deubiquitinate PML/RARα (Fig. 3F), confirming the importance of YOD1 catalytic activity to PML/RARα deubiquitination. Similar results were also observed in *in vitro* deubiquitination experiment with all four drug-resistant PML/RARα mutants (ΔF286, R276Q, L218P and A216V) (Fig. 3G). Collectively, these results clearly demonstrate that YOD1 interacts with PML/RARα and functions as the deubiquitinase of PML/RARα to regulate its protein stabilization. Moreover, the evident deubiquitinating effect of YOD1 on drug-resistant mutants suggests that current drug-resistant mutational hotspots within PML/RARα does not interfere with its deubiquitination by YOD1.

3.4. *Depletion of YOD1 leads to effective APL eradication in vitro and in vivo*

Considering the observations that inhibiting YOD1 promotes proteasomal degradation of PML/RARα, we further assessed whether targeting YOD1 could arrest APL progression. First, two shRNAs targeting YOD1 were introduced into NB4 cells (Fig. 4A). Because PML/RARα promotes the proliferation of APL cells, we first determined the antiproliferative effect of shYOD1 on APL cells. Notably, YOD1 knockdown potently inhibited the proliferation (Fig. 4B) and colony formation ability (Fig. 4C) of NB4 cells. Meanwhile, PML/RARα is also known to protect APL cells from apoptosis and acts as a transcriptional repressor of RARα-target genes to block myeloid differentiation[33,34]. Therefore, we detected the effects of shYOD1 on APL cell apoptosis and cell differentiation. We found that YOD1 depletion induced significant apoptosis of NB4 cells (Fig. 4D). Surprisingly, YOD1 depletion did not induce obvious apoptosis in non-APL AML cell lines (U937 and HL60) (Supporting Information Fig. S2A). Additionally, shYOD1 also significantly promoted CD11b expression in NB4 cells, which is a typical differentiation marker[35,36], but the CD11b expression of U937 and HL60 cell lines did not increase upon YOD1 knock down (Fig. S2B). These results indicate that silencing YOD1 in APL cells can suppress cell proliferation, induce cell apoptosis and cell differentiation in a PML/RARα-dependent manner.

Next, to confirm that YOD1 could be an effective therapeutic target in AML, we evaluated the effect of YOD1 inhibition on normal human hematopoietic stem cells (HSCs). The results demonstrate that YOD1 depletion showed little cytotoxicity in HSCs (Fig. S2C), which demonstrating the low potential toxic and side effects of targeting YOD1 and further supporting the hypothesis that targeting YOD1 may be a promising treatment of APL patients.

Then we further assessed the influence of YOD1 knockdown in drug-resistant APL cells. Genetic depletion of YOD1 was performed with shYOD1 (#1 and #2) in two drug-resistant APL cell strains (NB4R1 and NB4R2 cells) (Fig. 4E). Surprisingly, when transduced with shYOD1 lentivirus, most drug-resistant NB4R1 and NB4R2 cells lost the ability to proliferate and only multiplied twice in 5 days, whose proliferation rates were much lower than that transduced with shCtrl lentivirus (Fig. 4F). Similarity, the colony formation abilities of NB4R1 and NB4R2 cells were significantly suppressed by shYOD1 (Fig. 4G). Moreover, the numbers of apoptotic NB4R1 and NB4R2 cells were also remarkably increased by shYOD1 treatment (Fig. 4H). Taken together, these data validate that depletion of YOD1 exhibits strong suppressive effect on both APL and drug-resistant APL cells.

Furthermore, to test whether the suppressive activity of shYOD1 in APL cells could be reproduced *in vivo*, we utilized the APL xenograft mouse model. First, NB4 cells transduced with lentivirus containing shCtrl and shYOD1 (#1 and #2) were intravenously transplanted into NOD/SCID mice. When the shCtrl leukemic mice were moribund, we sacrificed three mice in each group to detect the APL burden in bone marrow. The morphological analysis of bone marrow cells showed that leukemic blasts were apparent in the shCtrl group, while they were rare in the shYOD1 groups (Fig. 4I). Moreover, we detected the population of $hCD45^{+}mCD45^{-}$ cells in the bone marrow, which directly reflected the overall leukemic burden. Strikingly, the proportion of $hCD45^{+}mCD45^{-}$ cells in the shCtrl group significantly increased (>1%), while these cells remained undetected (<1%) in the shYOD1 groups (Fig. 4J). Thus, both morphological analysis and proportion of $hCD45^{+}mCD45^{-}$ demonstrate that YOD1 knockdown reduces the human APL burden in leukemic mice. Furthermore, all the shCtrl leukemic mice died rapidly within 1 month, while the overall survival time was dramatically prolonged in the shYOD1 (#1 and #2) groups (Fig. 4K). More importantly, similar therapeutic effects of shYOD1 were also observed in NB4R1 xenograft mice, as assessed by reduced APL burden (Fig. 4L and M) and prolonged overall survival time (Fig. 4N). Collectively, these results demonstrate that shYOD1 represses the invasion of leukemic blasts in both APL and drug-resistant APL xenograft models, further supporting that YOD1 is a promising therapeutic target for APL, particularly for drug-resistant APL treatment.

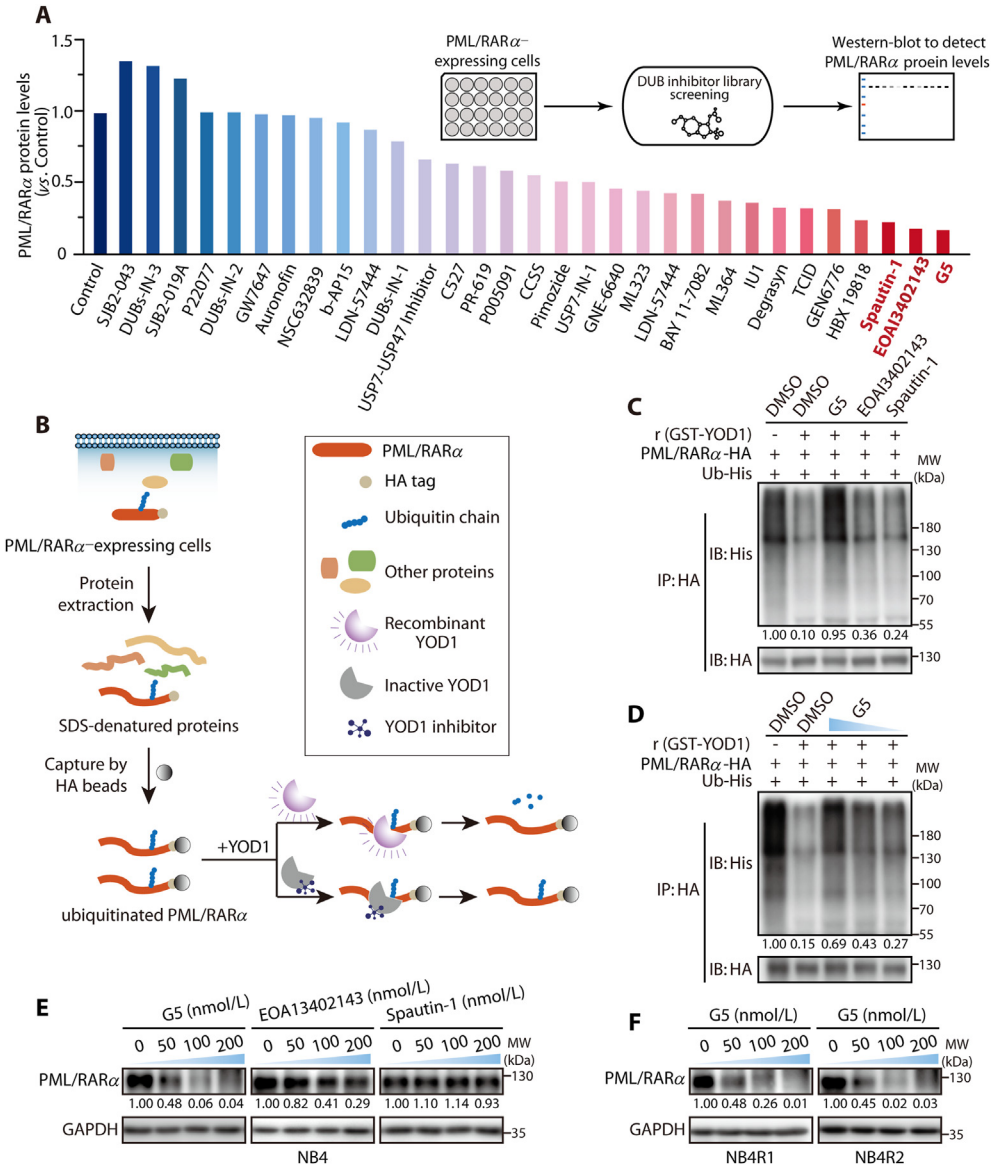

Figure 5 G5 inhibits the deubiquitination activity of YOD1 and triggers PML/RARα degradation. (A) Relative protein level of PML/RARα in the screening of DUB inhibitors. H1299 cells stably expressing PML/RARα were treated with the library of 28 reported DUB inhibitors at a concentration of 5 μmol/L for 12 h as indicated, and then, the protein levels of PML/RARα were assessed by Western blotting. (B) Schematic diagram of YOD1 activity detection after treatment with compounds *in vitro*. Ubiquitinated PML/RARα was immunoprecipitated from COS-7 cells transfected with PML/RARα-HA and His-Ub plasmids with after 10 μmol/L MG132 treatment. Recombinant GST-YOD1 was pretreated with DUB inhibitors for 1 h and subsequently incubated with ubiquitinated PML/RARα for 6 h. Then, the ubiquitylation level of PML/RARα was evaluated. (C) The deubiquitinating effect of YOD1 on PML/RARα upon DUB inhibitors. Recombinant GST-YOD1 was exposed to 10 μmol/L G5, EOAI3402143 or spautin-1 and then incubated with ubiquitinated PML/RARα. The ubiquitylation level of PML/RARα was evaluated. (D) The deubiquitinating effect of YOD1 on PML/RARα upon treatment with different concentrations of G5. GST-YOD1 was exposed to 5, 2.5 and 1.25 μmol/L G5 and then incubated with ubiquitinated PML/RARα. The ubiquitylation level of PML/RARα was measured. (E) Protein level of PML/RARα in NB4 cells after treatment with G5, EOAI3402143 and spautin-1 at concentrations of 0, 50, 100, and 200 nmol/L. (F) Protein level of PML/RARα in NB4R1 and NB4R2 cells after treatment with G5 at concentrations of 0, 50, 100, and 200 nmol/L. (C)−(F) Data are performed at least three individual experiments and one representative image is shown.

3.5. G5 inhibits the deubiquitination activity of YOD1 and triggers PML/RARα degradation

Since our data indicate that targeting YOD1 induces enzyme-dependent degradation of PML/RARα, we were inspired to apply a YOD1 inhibitor to eliminate PML/RARα for APL treatment. However, no small-molecule inhibitor of YOD1 has been reported to data. In order to give priority to the degradation effect of possible inhibitors on PML/RARα, we screened small molecules based on the level of PML/RARα protein. As shown in Fig. 5A and Supporting Information Fig. S3, we added a library of 31 reported DUB inhibitors to cells that stably expressed PML/RARα and then measured their effect on the protein level of PML/RARα. Three inhibitors (G5, EOAI3402143 and spautin-1) were found to

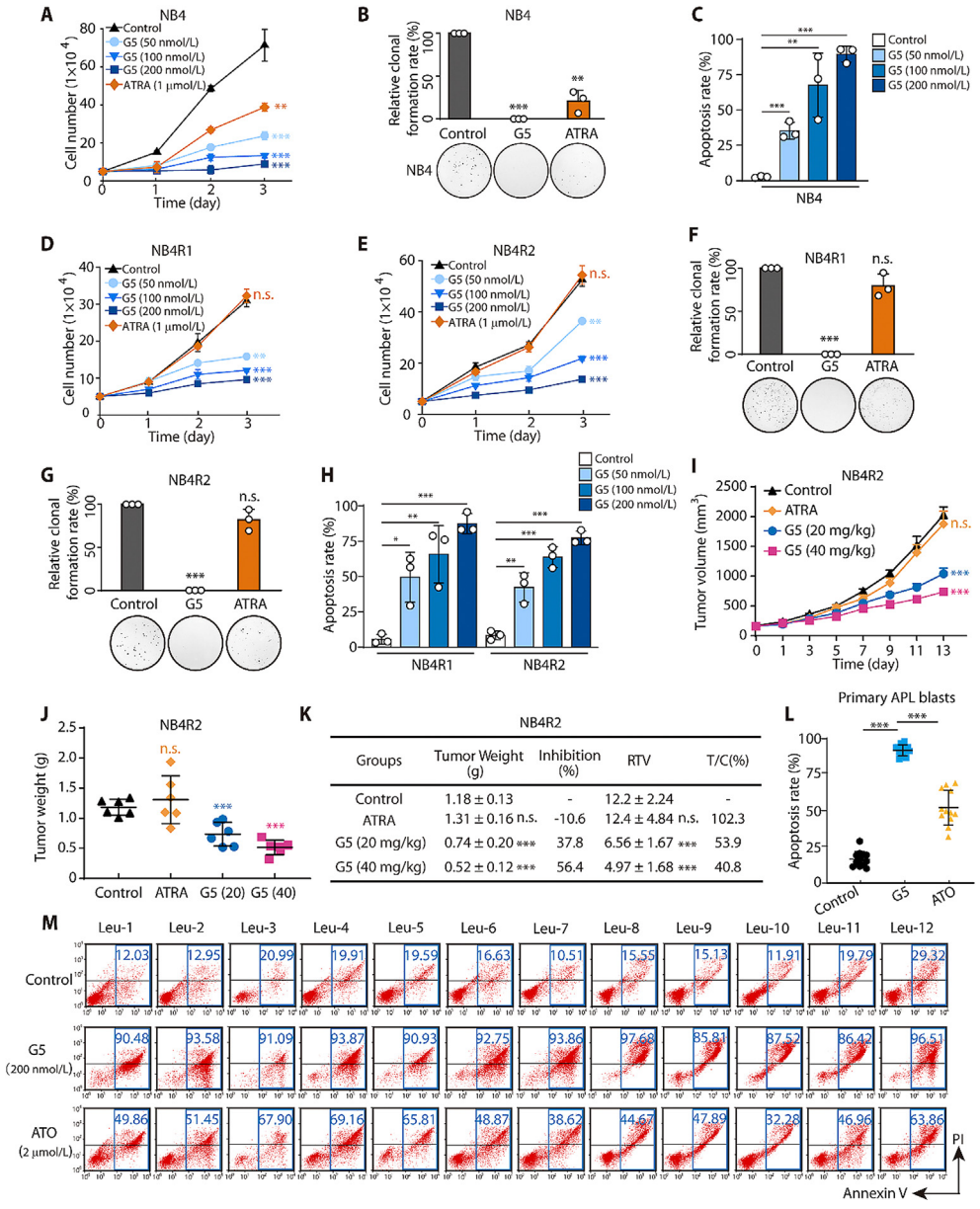

Groups	Tumor Weight (g)	Inhibition (%)	RTV	T/C(%)
Control	1.18 ± 0.13	-	12.2 ± 2.24	-
ATRA	1.31 ± 0.16 n.s.	-10.6	12.4 ± 4.84 n.s.	102.3
G5 (20 mg/kg)	0.74 ± 0.20 ***	37.8	6.56 ± 1.67 ***	53.9
G5 (40 mg/kg)	0.52 ± 0.12 ***	56.4	4.97 ± 1.68 ***	40.8

Figure 6 G5 shows a strong inhibitory effect on APL to overcome resistance by targeting YOD1. (A) Proliferation of NB4 cells treated with G5 (0, 50, 100, and 200 nmol/L) and ATRA (1 μmol/L), as measured by trypan blue exclusion test for the indicated times. (B) Colony formation assay of NB4 cells treated with G5 (100 nmol/L) and ATRA (100 nmol/L). 1000 cells were seeded per well and the colony numbers were counted after several days. Relative clonal formation rate is the ratio of the number of clones in each group to the number of clones in the control group. (C) FACS quantification of apoptosis with PI^-/Annexin V^+ or PI^+/Annexin V^+ NB4 cells. The cells were treated with G5 (0, 50, 100, and 200 nmol/L) for 48 h. (D)−(E) Proliferation of NB4R1 and NB4R2 cells. The cells were treated with G5 (0, 50, 100, and 200 nmol/L) and ATRA (1 μmol/L), and a trypan blue exclusion test was performed for the indicated times. (F)−(G) Colony formation assay of NB4R1 and NB4R2 cells treated with G5 (100 nmol/L) and ATRA (100 nmol/L). 2000 cells were seeded per well and the colony numbers were counted after several days. Relative clonal formation rate is the ratio of the number of clones in each group to the number of clones in the control group. (H) FACS quantification of apoptosis with PI^-/Annexin V^+ or PI^+/Annexin V^+ NB4R1 and NB4R2 cells. The cells were treated with G5 (0, 50, 100, and 200 nmol/L) for 48 h. (A)−(H) Data are presented as mean ± SD ($n = 3$); n.s., $P > 0.05$, $^*P < 0.05$, $^{**}P < 0.01$, $^{***}P < 0.001$ *vs.* Control or indicated. The significance analysis was conducted by one-way ANOVA analysis. (I)−(K) The effect of G5 on tumor growth in an NB4R2 xenograft nude mouse model. NB4 xenografts were established by subcutaneous injection of cells into nude mice ($n = 6$). G5 (20 or 40 mg/kg) was administered to the mice by intravenous injection into the tail vein every other day. ATRA was administered by intragastric injection every other day. (I) Tumor growth of the NB4R2 xenografts. Tumor volume growth curves are based as mean ± SE. (J) Tumor weight of the NB4R2 xenografts on Day 13. Data are presented as mean ± SD. (K) Effects of G5 on tumor size and tumor weight at pre-dose and post-dose. RTV, relative tumor volume; T/C (%) = $RTV_{Treatment}/RTV_{control} \times 100$. Criteria for therapeutic activity: T/C (%), optimal growth inhibition <50 = effective. Data are represented as mean ± SD. (K)−(L) n.s., $P > 0.05$, $^{***}P < 0.001$ *vs.* Control. The significance analysis was conducted by one-way ANOVA. (L)−(M) FACS quantification of apoptosis with PI^-/Annexin V^+ or PI^+/Annexin V^+ primary APL cells. Primary APL cells derived from the peripheral blood of patients at diagnosis were treated with G5 (200 nmol/L) and ATO (2 μmol/L) for 72 h. Data are presented as mean ± SD ($n = 12$); $^{***}P < 0.001$ *vs.* indicated. The significance analysis was conducted by two-tailed unpaired Student's *t*-test.

dramatically reduce the PML/RARα protein level. Among them, G5 exhibited the greatest effect of lowering PML/RARα protein level.

Next, to determine whether the inhibitors-induced PML/RARα decline is dependent on YOD1, we conducted the *in vitro* deubiquitination assay. As displayed in Fig. 5B, recombinant YOD1 was pretreated with DUB inhibitors or DMSO and then incubated with ubiquitinated PML/RARα. Finally, the ubiquitination level of PML/RARα was measured. Results show that G5 significantly destroyed the YOD1-induced decline of PML/RARα ubiquitination level, suggesting that the deubiquitination activity of YOD1 was almost completely blocked by G5 (Fig. 5C). By contrast, EOAI3402143 and spautin-1 did not affect the deubiquitination activity of YOD1 on the PML/RARα, indicating that they may affect the stability of PML/RARα through other mechanisms. Moreover, the inhibitory effect of G5 on the deubiquitination activity of YOD1 was concentration-dependent (Fig. 5D), further indicating G5 as a potent inhibitor of YOD1.

Finally, we then evaluated whether G5 could trigger the degradation of endogenous wild-type PML/RARα and its drug-resistant mutants. Results show that G5 potently reduced PML/RARα protein in NB4 cells, while EOAI3402143 slightly affected PML/RARα protein levels and spautin-1 exhibited no effect at the same concentrations (Fig. 5E). More encouragingly, G5 also triggered the strong degradation of mutated PML/RARα in NB4R1 and NB4R2 cells (Fig. 5F). Together, these data demonstrate that G5 promises to be an effective YOD1 inhibitor to induce PML/RARα degradation by inhibiting the deubiquitination activity of YOD1.

3.6. G5 shows a strong inhibitory effect on APL to overcome resistance by targeting YOD1

Since G5 was shown to drive PML/RARα degradation by inhibiting YOD1, we next assessed the capacity of G5 to suppress APL and relieve drug resistance. Treatment with G5 at 50−200 nmol/L effectively impaired the proliferation of NB4 cells, with most cells losing the ability to multiply, while ATRA at 1 μmol/L showed only an approximate 50% suppressive effect on NB4 cells (Fig. 6A). Moreover, G5 destroyed most of the clonal formation ability of NB4 cells with higher efficiency than ATRA (Fig. 6B). In addition, G5 potently induced apoptosis of NB4 cells in a concentration-dependent manner (Fig. 6C). Then, we attempted to identify the inhibitory effect of G5 on drug-resistant APL cells. Compared with the little suppressive ability of ATRA, G5 dramatically decreased the proliferation capacity of both the NB4R1 and NB4R2 cell lines (Fig. 6D and E). Similar results were obtained in the colony formation assay. G5 decreased the colony number of drug-resistant APL cells (NB4R1 and NB4R2), while ATRA failed to reduce their colony number (Fig. 6F and G). In addition, significant apoptosis of these drug-resistant APL cells was also observed upon G5 treatment (Fig. 6H). Furthermore, we evaluated the *in vivo* antitumor activity of G5 in a NB4R2 xenograft nude mouse model. G5 administration significantly inhibited tumor growth by 37.8% (20 mg/kg) and 56.4% (40 mg/kg) compared to the control, while ATRA showed no inhibitory effect. Moreover, G5 (40 mg/kg) exhibited effective therapeutic activity, as indicated by a T/C value of 40.8% (Fig. 6I−K). These results indicate that G5 exhibits strong suppressive effect in APL, particularly drug resistant APL.

Compared with immortalized cell lines, the primary APL blasts directly extracted from the bone marrow of patients were assessed to provide further evidence of G5 effectiveness. Thus, the effect of G5 was ultimately tested in 12 primary APL samples. When treated with G5, primary APL blasts underwent significant apoptosis ($91.71 \pm 3.76\%$; $P < 0.001$; $n = 12$). By contrast, as the clinical proapoptotic APL drug, ATO could only induce the highest apoptosis rate of ∼60%, and some APL blasts were even insensitive to ATO treatment (Fig. 6L and M). Notably, G5 caused the obvious apoptosis of primary APL at a very low concentration (200 nmol/L), while ATO was administered at a concentration 10-fold higher than that of G5 (2 μmol/L). In summary, our findings collectively show that targeting YOD1 by G5 leads to remarkable arrest of APL progression, providing a potential therapeutic agent for APL, particularly drug-resistant APL patients.

4. Discussion

Currently, ATRA/ATO with chemotherapy is the standard of care for APL, which still remaining hurdles including serious adverse events and drug resistance[6,8]. For ATRA/ATO-sensitive APL patients, once side effects occurred too severely to continue treatment. Our study validates YOD1 as a potential therapeutic target for APL, thus new compounds (such as YOD1 inhibitors) may well be the choice for such patients. More importantly, there are currently no drugs available for ATRA/ATO-resistant APL patients. Our results show that depletion of YOD1 exhibits strong suppressive effect on drug-resistant APL cells *in vitro* and *in vivo*, indicating that YOD1 is a promising therapeutic target for drug-resistant APL treatment.

Most fusion proteins, including PML/RARα, are recognized as major drivers of human tumorigenesis[37,38]. Due to their powerful roles in tumorigenesis and development, oncofusion proteins are ideal therapeutic targets[1,39]. But there still remain many challenges in targeting oncofusion proteins. On the one hand, tyrosine kinase oncofusions are considered druggable by kinase inhibitors, but prolonged treatment always leads to mutation-mediated acquired drug-resistance[40]. On the other hand, transcription factor oncofusions are difficult to target directly[41]. Notably, DUB dysregulation has been found to contribute to abnormal accumulation of various cancer-promoting proteins, such as MYC[26], KRAS[42], yes-associated protein (YAP) and transcriptional co-activator with PDZ-binding motif (TAZ)[43] and murine double minute 2 (MDM2)[44]. Thus, we hypothesized that degrading oncofusion proteins by targeting DUB could be a promising therapeutic strategy for oncofusion-driven tumors. Studies have confirmed the role of DUBs in regulating the stability of some oncofusion proteins, including promyelocytic leukemia zinc finger/retinoic acid receptor α (PLZF/RARα)-USP37[45] and internal tandem duplication within FLT3 (FLT3/ITD)-USP10[46]. Our study indicates that YOD1, the specific DUB of PML/RARα, is a key factor to maintain PML/RARα stability. Inhibiting YOD1 triggers significant clearance of the PML/RARα oncoprotein, thus ultimately exerts a therapeutic effect on APL. This discovery sets a great example for the realization of oncofusion protein degradation by targeting DUBs as a practicable therapeutic strategy in oncofusion-driven tumors.

Studies have proposed that YOD1 is involved in several biological activities in mammalian cells, including endoplasmic reticulum-associated degradation (EARD)[47], the clearance of damaged lysosomes[48] and antigen cross-presentation[49]. Moreover, YOD1 is closely associated with cancers. YOD1 is highly expressed in human liver cancer tissue and promotes cell migration and colony formation. Mechanistically, YOD1 regulates the hippo signaling pathway by regulating the ubiquitination level of

the ubiquitin ligase ITCH targeting large tumor suppressor kinase (LATS)[50]. These studies demonstrate the oncogenic function of YOD1 and indicate that YOD1 is a potential target for hepatic carcinoma. However, the functions of YOD1 in other cancers require further studies. Our current study identifies PML/RARα as a new substrate of YOD1 and indicates YOD1 as an appropriate target for APL treatment. Importantly, we have proved both the specificity and safety of targeting YOD1 by evaluating the effects on non-APL cell lines and normal human HSCs, which showed little cytotoxicity due to lack of PML/RARα (Fig. S2). Additionally, Dai et al.[51] constructed *Yod1* gene knockout (KO) mice and found that the *Yod1*-KO mice bore pups normally without embryonic lethality, and no significant pathological phenotype was observed in the *Yod1*-KO mice. These studies may suggest the relative safety of inhibiting YOD1. Taken together, our results indicate that YOD1 can be a potential drug target for treating APL.

Most DUBs contain catalytically active cysteine residues, making them highly possible to be intervened by small compounds. DUBs are classified into six families, including ubiquitin carboxyl terminal hydrolase (UCH) family, USP family, OTU family, Machado−Joseph domain-containing protease (MJD) family, Jab1/Pab1/MPN domain-containing protease (JAMM) family and motif-interacting with ubiquitin-containing novel DUB family (MINDY). However, the degree of research on DUB inhibitors varies considerably in different DUB families. The current studies on small-molecule inhibitors of DUBs mainly focus on UCH family and USP family, rather than OTU family[24]. Notably, OTU family is Ub linkage-specific[52], which indicates the relatively small probability of mutual compensation among different OTUs, even though they show structural similarity. Therefore, OTU inhibitors, such as YOD1 inhibitors, may exhibit higher efficiency than other DUB family inhibitors. In this work, we generated a screening model based on the stability of PML/RARα and speculated that G5 would be the first YOD1 inhibitor and the first OTU inhibitor.

A previous study revealed that G5 targeted the ubiquitin-proteasome system by inhibiting ubiquitin isopeptidases[53]. Later, G5 was identified to target the deubiquitinating activity of BRCC3 and subsequently inhibited NLRP3 inflammasome activation[54,55]. G5 has also been reported to induce the apoptosis of IMR90-E1A human fibroblasts at a concentration of 1.25 μmol/L and apoptosis-resistant double-deficient BAX/BAK (DKO) mouse embryo fibroblasts at a concentration of 5 μmol/L[56]. However, there is no current research that directly investigates the possible role of G5 in tumor cells. Our results reveal the obvious suppressive effect of G5 on leukemia cells for the first time. Notably, the concentration of G5 (200 nmol/L) to induce APL cell apoptosis was found to be much lower than that needed to induce normal cell apoptosis. More importantly, because of the obvious inhibitory effects of G5 on drug-resistant APL, our work indicates that G5 may be effective in overcoming APL drug resistance.

5. Conclusions

In summary, our study provides new insights into the function of YOD1 in APL progression by deubiquitinating and stabilizing the PML/RARα oncoprotein. Then we demonstrate that suppression of YOD1 by shRNA or its newfound inhibitor G5 triggers the degradation of PML/RARα to inhibit drug-resistant APL both *in vitro* and *in vivo*. Taken together, our study not only reveal the DUB-related regulatory mechanism on ubiquitination degradation of PML/RARα and validate YOD1 as a potential therapeutic target for APL, but also suggest G5 as a YOD1 inhibitor to be the promising candidate to cure APL, particularly drug-resistant APL patients.

Acknowledgments

Dr. Lingtao Wu (University of Southern California, USA) kindly donated NB4 cell line. NB4R1 cells were kindly gifted from Dr. He Huang (Zhejiang University, Hangzhou, China) and NB4R2 were kindly provided by Dr. Jian Zhang (Shanghai Jiao Tong University, Shanghai, China). This work was supported by grants from the National Natural Science Foundation of China (No. 81973354 to Meidan Ying), China Postdoctoral Science Foundation (No. 2020T130593 to Xuejing Shao), Leading Talent of "Ten Thousand Plan"-National High-Level Talents Special Support Plan and the Fundamental Research Funds for the Central Universities (China).

Author contributions

Meidan Ying and Xuejing Shao conceived the study and analyzed data; Meidan Ying, Xuejing Shao, Yingqian Chen and Wenxin Du wrote the manuscript. Xuejing Shao and Yingqian Chen performed dual-luciferase reporter system screening and cell-based YOD1 inhibitor screening assay; Xuejing Shao, Yingqian Chen, Shaowei Bing and Wenxin Du performed the immunoprecipitation and Western blotting procedure; Yingqian Chen and Wei Wang performed the *in vitro* ubiquitination assay; Yingqian Chen, Wei Wang, Xingya Zhang and Minyi Cai performed the cellular proliferation analysis, soft agar formation assay and cell apoptosis assay; Xuejing Shao, Yingqian Chen and Wei Wang performed the animal studies; Ji Cao, Xiaojun Xu, Qiaojun He and Bo Yang conceived the experiments and helped organize the paper.

Conflicts of interest

The authors declare no conflicts of interest.

Appendix A. Supporting information

Supporting data to this article can be found online at https://doi.org/10.1016/j.apsb.2021.10.020.

References

1. de Thé H, Pandolfi PP, Chen Z. Acute promyelocytic leukemia: a paradigm for oncoprotein-targeted cure. *Cancer Cell* 2017;**32**:552−60.
2. Brown D, Kogan S, Lagasse E, Weissman I, Alcalay M, Pelicci PG, et al. A PMLRARalpha transgene initiates murine acute promyelocytic leukemia. *Proc Natl Acad Sci U S A* 1997;**94**:2551−6.
3. Grisolano JL, Wesselschmidt RL, Pelicci PG, Ley TJ. Altered myeloid development and acute leukemia in transgenic mice expressing PML-RAR alpha under control of cathepsin G regulatory sequences. *Blood* 1997;**89**:376−87.
4. Nasr R, Guillemin MC, Ferhi O, Soilihi H, Peres L, Berthier C, et al. Eradication of acute promyelocytic leukemia-initiating cells through PML-RARA degradation. *Nat Med* 2008;**14**:1333−42.
5. Sanz MA, Fenaux P, Tallman MS, Estey EH, Lowenberg B, Naoe T, et al. Management of acute promyelocytic leukemia: updated recommendations from an expert panel of the European LeukemiaNet. *Blood* 2019;**133**:1630−43.

6. Lo-Coco F, Avvisati G, Vignetti M, Thiede C, Orlando SM, Iacobelli S, et al. Retinoic acid and arsenic trioxide for acute promyelocytic leukemia. *N Engl J Med* 2013;**369**:111−21.
7. Girmenia C, Lo Coco F, Breccia M, Latagliata R, Spadea A, D'Andrea M, et al. Infectious complications in patients with acute promyelocytic leukaemia treated with the AIDA regimen. *Leukemia* 2003;**17**:925−30.
8. Wang QQ, Hua HY, Naranmandura H, Zhu HH. Balance between the toxicity and anticancer activity of arsenic trioxide in treatment of acute promyelocytic leukemia. *Toxicol Appl Pharmacol* 2020;**409**:115299.
9. Madan V, Shyamsunder P, Han L, Mayakonda A, Nagata Y, Sundaresan J, et al. Comprehensive mutational analysis of primary and relapse acute promyelocytic leukemia. *Leukemia* 2016;**30**:1672−81.
10. Liu J, Zhu HH, Jiang H, Jiang Q, Huang XJ. Varying responses of PML-RARA with different genetic mutations to arsenic trioxide. *Blood* 2016;**127**:243−50.
11. Goto E, Tomita A, Hayakawa F, Atsumi A, Kiyoi H, Naoe T. Missense mutations in PML-RARA are critical for the lack of responsiveness to arsenic trioxide treatment. *Blood* 2011;**118**:1600−9.
12. Li K, Wang F, Cao WB, Lv XX, Hua F, Cui B, et al. TRIB3 promotes APL progression through stabilization of the oncoprotein PML-RARα and inhibition of p53-mediated senescence. *Cancer Cell* 2017;**31**: 697−710.e7.
13. Lallemand-Breitenbach V, Jeanne M, Benhenda S, Nasr R, Lei M, Peres L, et al. Arsenic degrades PML or PML-RARα through a SUMO-triggered RNF4/ubiquitin-mediated pathway. *Nat Cell Biol* 2008;**10**:547−55.
14. Zhang XW, Yan XJ, Zhou ZR, Yang FF, Wu ZY, Sun HB, et al. Arsenic trioxide controls the fate of the PML-RARα oncoprotein by directly binding PML. *Science* 2010;**328**:240−3.
15. Lallemand-Breitenbach V, Zhu J, Chen Z, de Thé H. Curing APL through PML/RARA degradation by As_2O_3. *Trends Mol Med* 2012;**18**:36−42.
16. Zhu J, Gianni M, Kopf E, Honore N, Chelbi-Alix M, Koken M, et al. Retinoic acid induces proteasome-dependent degradation of retinoic acid receptor alpha (RARα) and oncogenic RARα fusion proteins. *Proc Natl Acad Sci U S A* 1999;**96**:14807−12.
17. Isakson P, Bjoras M, Boe SO, Simonsen A. Autophagy contributes to therapy-induced degradation of the PML/RARA oncoprotein. *Blood* 2010;**116**:2324−31.
18. Shima Y, Honma Y, Kitabayashi I. PML-RARα and its phosphorylation regulate PML oligomerization and HIPK2 stability. *Cancer Res* 2013;**73**:4278−88.
19. Gianni M, Terao M, Kurosaki M, Paroni G, Brunelli L, Pastorelli R, et al. S100A3 a partner protein regulating the stability/activity of RARα and PML-RARα in cellular models of breast/lung cancer and acute myeloid leukemia. *Oncogene* 2019;**38**:2482−500.
20. Chen ZH, Wang WT, Huang W, Fang K, Sun YM, Liu SR, et al. The lncRNA HOTAIRM1 regulates the degradation of PML-RARA oncoprotein and myeloid cell differentiation by enhancing the autophagy pathway. *Cell Death Differ* 2017;**24**:212−24.
21. Zeng CW, Chen ZH, Zhang XJ, Han BW, Lin KY, Li XJ, et al. MIR125B1 represses the degradation of the PML-RARA oncoprotein by an autophagy−lysosomal pathway in acute promyelocytic leukemia. *Autophagy* 2014;**10**:1726−37.
22. Clague MJ, Urbe S, Komander D. Breaking the chains: deubiquitylating enzyme specificity begets function. *Nat Rev Mol Cell Biol* 2019; **20**:338−52.
23. Mevissen TET, Komander D. Mechanisms of deubiquitinase specificity and regulation. *Annu Rev Biochem* 2017;**86**:159−92.
24. Harrigan JA, Jacq X, Martin NM, Jackson SP. Deubiquitylating enzymes and drug discovery: emerging opportunities. *Nat Rev Drug Discov* 2018;**17**:57−78.
25. Tavana O, Li D, Dai C, Lopez G, Banerjee D, Kon N, et al. HAUSP deubiquitinates and stabilizes N-Myc in neuroblastoma. *Nat Med* 2016;**22**:1180−6.
26. Popov N, Wanzel M, Madiredjo M, Zhang D, Beijersbergen R, Bernards R, et al. The ubiquitin-specific protease USP28 is required for MYC stability. *Nat Cell Biol* 2007;**9**:765−74.
27. Liu S, Gonzalez-Prieto R, Zhang M, Geurink PP, Kooij R, Iyengar PV, et al. Deubiquitinase activity profiling identifies UCHL1 as a candidate oncoprotein that promotes TGFβ-induced breast cancer metastasis. *Clin Cancer Res* 2020;**26**:1460−73.
28. Ying M, Shao X, Jing H, Liu Y, Qi X, Cao J, et al. Ubiquitin-dependent degradation of CDK2 drives the therapeutic differentiation of AML by targeting PRDX2. *Blood* 2018;**131**:2698−711.
29. Cheung AM, Wan TS, Leung JC, Chan LY, Huang H, Kwong YL, et al. Aldehyde dehydrogenase activity in leukemic blasts defines a subgroup of acute myeloid leukemia with adverse prognosis and superior NOD/SCID engrafting potential. *Leukemia* 2007;**21**:1423−30.
30. Gill S, Tasian SK, Ruella M, Shestova O, Li Y, Porter DL, et al. Preclinical targeting of human acute myeloid leukemia and myeloablation using chimeric antigen receptor-modified T cells. *Blood* 2014;**123**:2343−54.
31. Kim JA, Shim JS, Lee GY, Yim HW, Kim TM, Kim M, et al. Microenvironmental remodeling as a parameter and prognostic factor of heterogeneous leukemogenesis in acute myelogenous leukemia. *Cancer Res* 2015;**75**:2222−31.
32. Ruchaud S, Duprez E, Gendron MC, Houge G, Genieser HG, Jastorff B, et al. Two distinctly regulated events, priming and triggering, during retinoid-induced maturation and resistance of NB4 promyelocytic leukemia cell line. *Proc Natl Acad Sci U S A* 1994;**91**:8428−32.
33. Rousselot P, Hardas B, Patel A, Guidez F, Gaken J, Castaigne S, et al. The PML-RAR alpha gene product of the t(15;17) translocation inhibits retinoic acid-induced granulocytic differentiation and mediated transactivation in human myeloid cells. *Oncogene* 1994;**9**: 545−51.
34. Nason-Burchenal K, Takle G, Pace U, Flynn S, Allopenna J, Martin P, et al. Targeting the PML/RAR alpha translocation product triggers apoptosis in promyelocytic leukemia cells. *Oncogene* 1998;**17**:1759−68.
35. Drayson MT, Michell RH, Durham J, Brown G. Cell proliferation and CD11b expression are controlled independently during HL60 cell differentiation initiated by 1,25α-dihydroxyvitamin D_3 or all-*trans*-retinoic acid. *Exp Cell Res* 2001;**266**:126−34.
36. Tasseff R, Jensen HA, Congleton J, Dai D, Rogers KV, Sagar A, et al. An effective model of the retinoic acid induced HL-60 differentiation program. *Sci Rep* 2017;**7**:14327.
37. Cocco E, Scaltriti M, Drilon A. NTRK fusion-positive cancers and TRK inhibitor therapy. *Nat Rev Clin Oncol* 2018;**15**:731−47.
38. Davies KD, Doebele RC. Molecular pathways: ROS1 fusion proteins in cancer. *Clin Cancer Res* 2013;**19**:4040−5.
39. Khotskaya YB, Holla VR, Farago AF, Mills Shaw KR, Meric-Bernstam F, Hong DS. Targeting TRK family proteins in cancer. *Pharmacol Ther* 2017;**173**:58−66.
40. Zhu VW, Klempner SJ, Ou SI. Receptor tyrosine kinase fusions as an actionable resistance mechanism to EGFR TKIs in EGFR-mutant non-small-cell lung cancer. *Trends Cancer* 2019;**5**:677−92.
41. Erkizan HV, Uversky VN, Toretsky JA. Oncogenic partnerships: EWS−FLI1 protein interactions initiate key pathways of Ewing's sarcoma. *Clin Cancer Res* 2010;**16**:4077−83.
42. Mustachio LM, Lu Y, Tafe LJ, Memoli V, Rodriguez-Canales J, Mino B, et al. Deubiquitinase USP18 loss mislocalizes and destabilizes KRAS in lung cancer. *Mol Cancer Res* 2017;**15**:905−14.
43. Zhu H, Yan F, Yuan T, Qian M, Zhou T, Dai X, et al. USP10 promotes proliferation of hepatocellular carcinoma by deubiquitinating and stabilizing YAP/TAZ. *Cancer Res* 2020;**80**:2204−16.
44. Zou Q, Jin J, Hu H, Li HS, Romano S, Xiao Y, et al. USP15 stabilizes MDM2 to mediate cancer-cell survival and inhibit antitumor T cell responses. *Nat Immunol* 2014;**15**:562−70.
45. Yang WC, Shih HM. The deubiquitinating enzyme USP37 regulates the oncogenic fusion protein PLZF/RARA stability. *Oncogene* 2013; **32**:5167−75.
46. Weisberg EL, Schauer NJ, Yang J, Lamberto I, Doherty L, Bhatt S, et al. Inhibition of USP10 induces degradation of oncogenic FLT3. *Nat Chem Biol* 2017;**13**:1207−15.
47. Ernst R, Mueller B, Ploegh HL, Schlieker C. The otubain YOD1 is a deubiquitinating enzyme that associates with p97 to facilitate protein dislocation from the ER. *Mol Cell* 2009;**36**:28−38.

48. Papadopoulos C, Kirchner P, Bug M, Grum D, Koerver L, Schulze N, et al. VCP/p97 cooperates with YOD1, UBXD1 and PLAA to drive clearance of ruptured lysosomes by autophagy. *EMBO J* 2017;**36**:135−50.
49. Sehrawat S, Koenig PA, Kirak O, Schlieker C, Fankhauser M, Ploegh HL. A catalytically inactive mutant of the deubiquitylase YOD-1 enhances antigen cross-presentation. *Blood* 2013;**121**:1145−56.
50. Kim Y, Kim W, Song Y, Kim JR, Cho K, Moon H, et al. Deubiquitinase YOD1 potentiates YAP/TAZ activities through enhancing ITCH stability. *Proc Natl Acad Sci U S A* 2017;**114**:4691−6.
51. Dai Hong-miao, Fu Ye-sheng, Zhang Ling-qiang. Construction of YOD1 knockout mice on CRISPR/Cas9 technology. *China Biotechnol* 2018;**38**:52−7.
52. Mevissen TE, Hospenthal MK, Geurink PP, Elliott PR, Akutsu M, Arnaudo N, et al. OTU deubiquitinases reveal mechanisms of linkage specificity and enable ubiquitin chain restriction analysis. *Cell* 2013;**154**:169−84.
53. Aleo E, Henderson CJ, Fontanini A, Solazzo B, Brancolini C. Identification of new compounds that trigger apoptosome-independent caspase activation and apoptosis. *Cancer Res* 2006;**66**:9235−44.
54. Py BF, Kim MS, Vakifahmetoglu-Norberg H, Yuan J. Deubiquitination of NLRP3 by BRCC3 critically regulates inflammasome activity. *Mol Cell* 2013;**49**:331−8.
55. Zhou L, Liu T, Huang B, Luo M, Chen Z, Zhao Z, et al. Excessive deubiquitination of NLRP3-R779C variant contributes to very-early-onset inflammatory bowel disease development. *J Allergy Clin Immunol* 2021;**147**:267−79.
56. Fontanini A, Foti C, Potu H, Crivellato E, Maestro R, Bernardi P, et al. The isopeptidase inhibitor G5 triggers a caspase-independent necrotic death in cells resistant to apoptosis: a comparative study with the proteasome inhibitor bortezomib. *J Biol Chem* 2009;**284**:8369−81.